6. Artificial Solar Eclipse

Experiment MA-148*

G. M. Nikolskiy,[a†] A. I. Simonov,[b] I. S. Kim,[a] R. T. Giuli,[c]
M. D. Jenness,[c] and A. N. Lunde[c]

ABSTRACT

On July 19, 1975, the Apollo spacecraft successfully occulted the solar disk from the field of view of a camera mounted in the Soyuz spacecraft while performing a spacecraft separation maneuver to permit the outer solar corona to be viewable by the Soyuz camera. The camera operated automatically, and 55 frames were developed for scientific analysis.

INTRODUCTION

The Artificial Solar Eclipse (ASE) Experiment is one of the five experiments that incorporated joint activities between the U.S. and U.S.S.R. crews during the Apollo-Soyuz Test Project (ASTP) mission. The objective of this experiment was to detect the extended region of the solar corona by photographing it from the Soyuz spacecraft against the black space background, while the disk of the Sun was occulted by the Apollo spacecraft. A secondary objective was to determine the distribution of contaminant gaseous and particle atmosphere around the Apollo spacecraft. The Apollo crew performed the required spacecraft maneuvers and photographed the eclipse shadow on the Soyuz vehicle, and the Soyuz crew photographed the corona. The ASE experiment and the method for conducting it were proposed by A. I. Simonov and G. M. Nikolskiy. The detailed trajectory computation was a joint effort of NASA and the U.S.S.R. Academy of Sciences.

OPERATIONS AND EQUIPMENT

The ASE was performed by separating the Apollo from the Soyuz shortly after orbital sunrise in such a way that Apollo occulted the Sun from view of the Soyuz orbital module (OM) hatch window. Apollo backed away from Soyuz toward the Sun to a separation distance (225 m) at which the apparent diameter of the Apollo command module (CM), as seen from Soyuz, was approximately 2 solar diameters. Apollo then reversed direction and performed an approach and docking maneuver with Soyuz. Apollo totally occulted the Sun during the separation maneuver, and Soyuz performed automatic sequence photography in the solar direction during the spacecraft separation and approach maneuvers. The orbital events are described in figure 6-1 and table 6-I. Before orbital sunrise, the Soyuz crew installed the corona-photography camera near the interior surface of the OM hatch window, looking out along the plus-X axis of the Soyuz vehicle. The frame

---

*The joint U.S.-U.S.S.R. designation was "Experiment AS-4."

[a]Institute of Terrestrial Magnetism, Ionosphere, and Radiowave Propagation, U.S.S.R. Academy of Sciences.

[b]Space Research Institute, U.S.S.R. Academy of Sciences.

[c]NASA Lyndon B. Johnson Space Center.

†Principal Investigator.

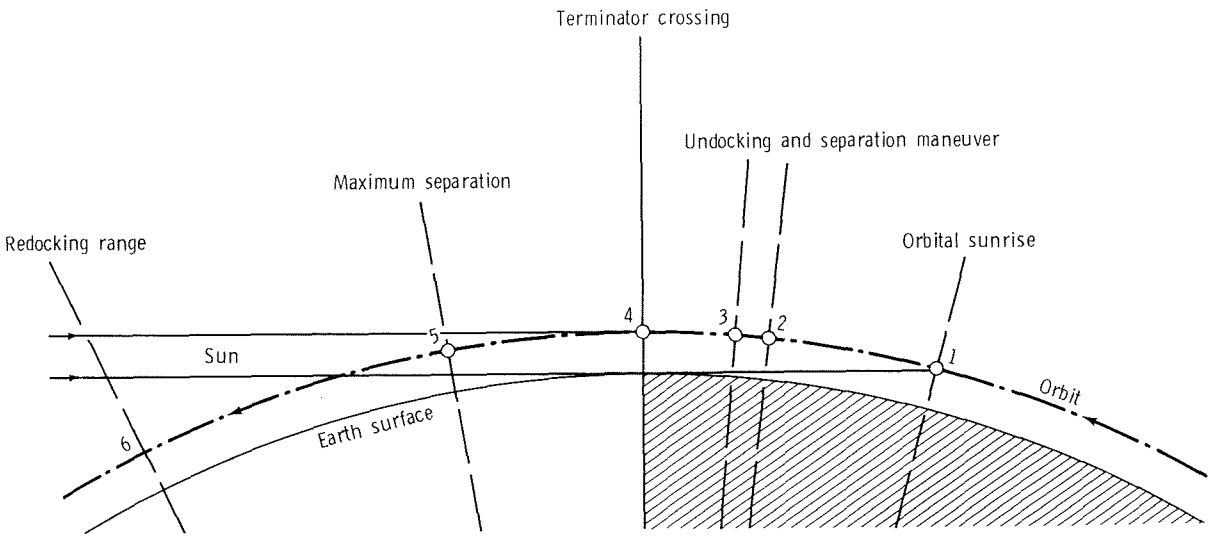

FIGURE 6-1.—Orbital schematic of artificial solar eclipse during the 57th orbit of the Apollo spacecraft and the 65th orbit of the Soyuz spacecraft. Numbers refer to events described in table 6-I.

TABLE 6-I.—Sequence of Events From First Undocking to Second Docking, July 19, 1975

Event	*UT, hr:min:sec*	*Spacecraft separation, m*	*Event description*
1	12:02:05	0	Orbit sunrise.
2	12:03:20	0	At undocking, spring release mechanism gives Soyuz a velocity of 0.10 m/sec along the Soyuz minus-X axis and gives Apollo a velocity of 0.05 m/sec along the Apollo minus-X axis.
	12:03:35	2.3	Apollo begins first 4-jet, minus-X, 0.38-m/sec separation maneuver (initiated after a 15-second coast period) along line of sight to Sun direction and maintains inertial attitude hold.
	12:03:38	3.3	Reaction control system (RCS) engines cut off.
	12:03:50	9.6	Apollo begins second 4-jet, minus-X, 0.50-m/sec separation maneuver after a 12-second coast period.
3	12:03:54	12.8	RCS engines cut off; separation rate, 1.03 m/sec.
4	12:05:55	137	The two spacecraft cross the Earth terminator.
5	12:07:20	225	Apollo begins a 2-m/sec, 4-jet, plus-X RCS maneuver to null the separation rate and return the Apollo vehicle to the redocking position.
	12:07:36	225	RCS engines cut off.
6	12:10:58	<17	Apollo achieves docking range and begins a 1-m/sec, 4-jet, minus-X RCS maneuver to null the closing velocity component.

size was 50 by 50 mm, the lens focal length was 90 mm, and the aperture ratio was 1:2.8. The photographs were taken in "white" light over the wavelength range of approximately 400 to 750 nm; the lens used no filter. The Kodak HS-2485 (70 mm) film was mounted in a mechanized-drive magazine on the back of the camera. A timer controlled the automated camera operation in continuously repeated cycles, with six exposures per cycle. Tables 6-II and 6-III give the timing data for the camera operation.

Before the spacecraft undocking, the Apollo crew installed a U.S.S.R. light baffle on the outside of the Soyuz OM hatch window. The baffle (fig. 6-2) shielded the hatch window from light reflected from the Soyuz docking mechanism and from the Earth. To block the intense sunlight reflected from the Earth beyond the terminator, the baffle design incorporated vignetting of the frame so that approximately one-half the frame toward the Earth was totally obscured (figs. 6-2 and 6-3).

Also during separation, the 16-mm Apollo data acquisition camera (DAC) was mounted in a CM window to view along the Apollo plus-X axis. The 75-mm focal length lens of the DAC automatically operated at 12 frames/sec, exposing SO-242 color film at 1/125 second. The purpose of the DAC photography was to monitor the motion of the umbra on the Soyuz spacecraft.

TABLE 6-II.—Interval Between Start of a Series and the Beginning of an Exposure Within the Series

Exposure no.	*Exposure time, sec*	*Interval, sec*
1	11	0
2	3.3	13.75
3	1.1	19.80
4	.33	23.65
5	.165	26.73
6	3.3	29.65

TABLE 6-III.—Interval Between the End of Undocking and the Start of a Series

Series	*Interval, sec*
I	20.7
II	56.4
III	92.1
IV	127.8
IX	306.3
X	342.0
XI	377.7
XII	413.4
XXI	734.7

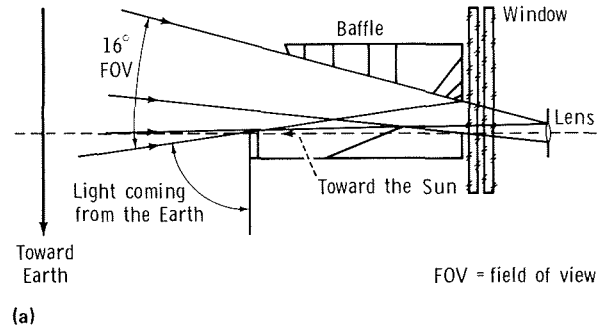

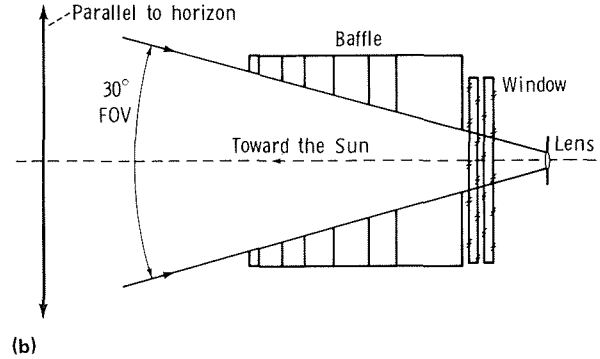

FIGURE 6-2.—Optical schematic of the baffle. (a) Side view. (b) Top view.

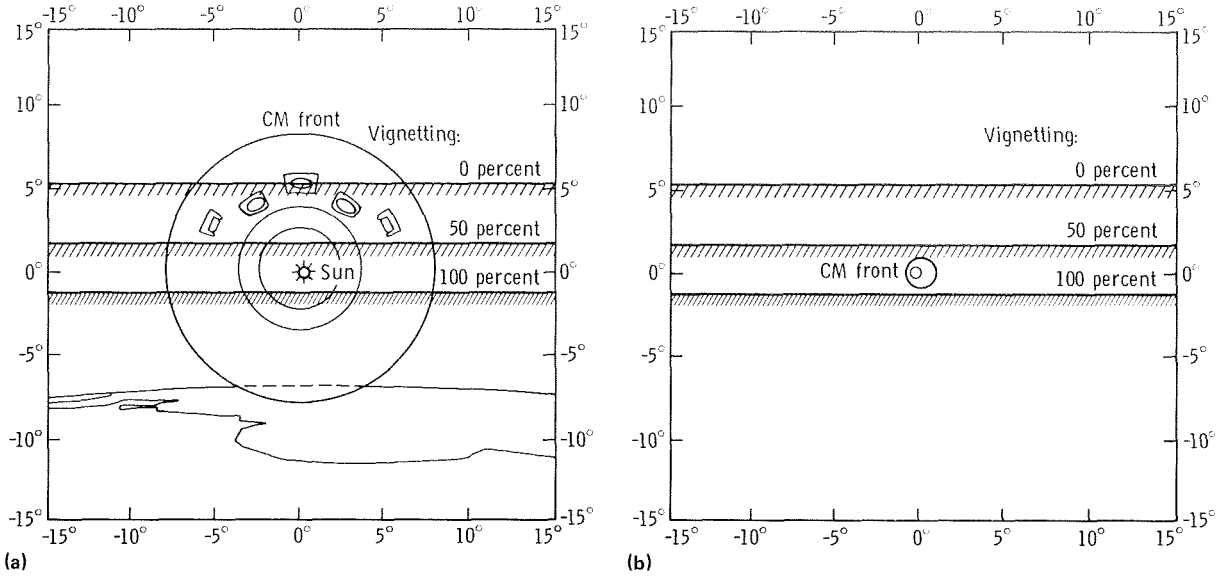

FIGURE 6-3.—View of the Apollo spacecraft as seen from the Soyuz spacecraft. The field of view is 30° with the Sun in the center of the view. The indicated vignetting is from the design of the light baffle on the Soyuz hatch window. (a) 12.8 m from Soyuz (after the second reaction control system (RCS) separation burn). (b) 225 m from Soyuz (just before the RCS approach burn).

DESCRIPTION OF PHOTOGRAPHS

Photographs taken during the ASE experiment were processed at the Solar Activity Laboratory in Moscow. The film processing used D-19 developer and a developing time of 12 minutes at a temperature of 298 K (25° C). Relative calibration was performed by means of a tube photometer, which produced 12 marks with relative intensities within 2.4 orders of magnitude. The calibration used an unexposed emulsion that had been flown onboard the Soyuz 19 spacecraft under conditions identical to those of the ASTP mission; calibration was performed with exposures of 10, 3, 1, and 0.3 seconds.

Fifty-three frames (series I to IV, IX to XII, and XXI) contain information on the illumination around the Apollo spacecraft. The outer corona (i.e., diffuse illumination) is more concentrated toward the ecliptic and is visible on 19 frames that were the least exposed to the reaction control system (RCS) exhaust illumination. Unfortunately, the glass of the Soyuz OM hatch window was also illuminated, apparently by light coming through the OM side window and by light from the instrument panel. The fact that frames were exposed in those portions that were fully shielded by the baffle indicates that the illumination came from the cabin. Optimum results were obtained with 0.16- and 0.33-second exposures; frames with longer exposures have high photographic density.

Three celestial objects (two stars, γ Geminorum and α Canis Minoris, and the planet Mercury) are visible on nearly all negatives; the frames view the portion of the sky that is southwest of the Sun. The photographic resolution is 2′ to 4′ (0.05 to 0.1 mm), depending on the location on the frame and exposure time. The resolution is determined by a combination of several factors such as the lens quality, the emulsion grain size, and the camera vibrations. Fully visible is a narrow ring around the Apollo spacecraft. The ring results from the diffraction of solar light and creates no background at distances of more than 0.5 m from the Apollo spacecraft periphery. The interference is fully accounted for by the illumination from the RCS exhaust and by the previously mentioned cabin illumination. Visible on many frames are not only the Apollo RCS engine plumes, which can reach as far as the

frame boundaries (at a spacecraft separation of 50 m), but also the particles escaping from the jet engines with a velocity of several meters per second.

SCALE AND SHADING DETERMINATION

For scale and shading determination, distances between stars were measured, and rectangular coordinates of the stars were calculated from the photographs. If x and y are the coordinates of the stars measured on the negatives from the solar disk center, perpendicular to and along the declination circle, respectively, then

$$\left.\begin{aligned} x &= \frac{\tan(\alpha - \alpha_\odot)\cos A}{\cos(A - \delta_\odot)} \\ y &= \tan(A - \delta_\odot) \end{aligned}\right\} \qquad (6\text{-}1)$$

where α and δ are the right ascension and declination, respectively, and the auxiliary angle A is

$$\tan A \equiv \frac{\tan \delta}{\cos(\alpha - \alpha_\odot)} \qquad (6\text{-}2)$$

A comparison of measurements with calculations indicated that the solar position on the negatives can be determined with 0.1 percent relative accuracy and that a more accurate value for the camera focal length is 90.4 mm.

Figure 6-4 shows the Apollo silhouette with respect to the Sun as seen from Soyuz at different times corresponding to different values of spacecraft separation d. The value of d is related to the apparent outer diameter d_A of Apollo as follows.

$$d = \frac{353.4}{d_A} - 5.8 \qquad (6\text{-}3)$$

where d is the distance in meters between the Soyuz camera lens and the front end of the docking module attached to Apollo and where d_A is measured on the negatives in millimeters. Measurements of d_A were made on 24 photographs, yielding d as a function of time for both

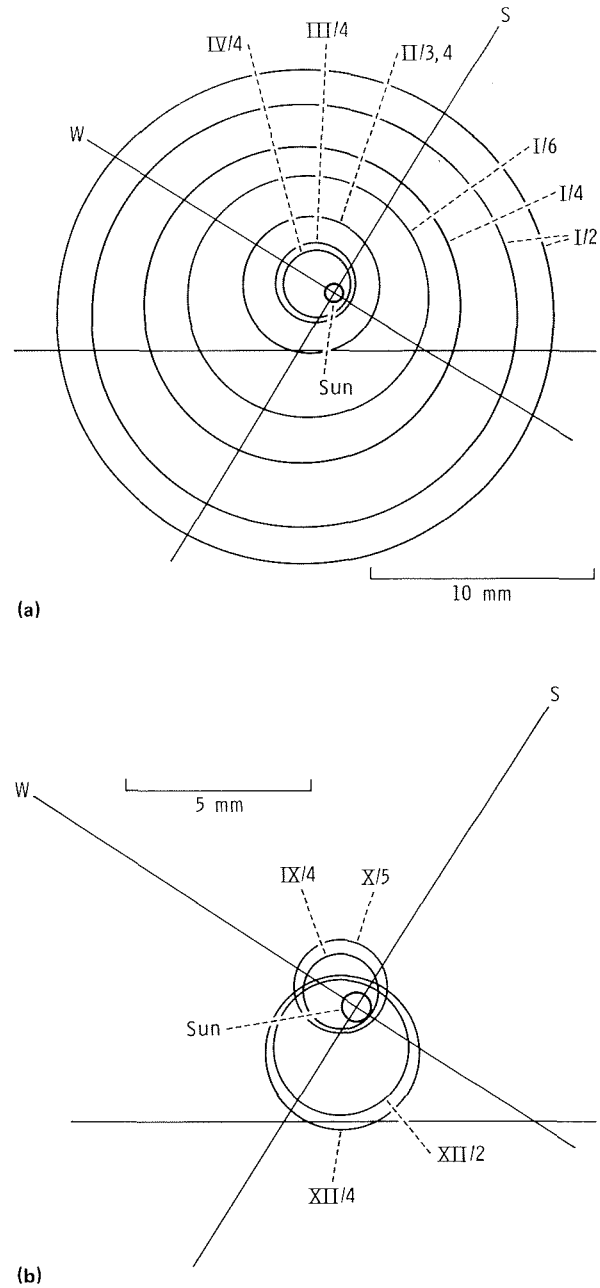

FIGURE 6-4.—Silhouette of the Apollo spacecraft with respect to the Sun (as seen on the frames indicated), corresponding to different values of d during the separation maneuver and during the approach maneuver. Shown are directions of the declination circle (S indicates south) and the orthogonal coordinate (W indicates west). Series numbers are given in Roman numerals and exposure numbers in Arabic numerals (e.g., IV/4). (a) Separation maneuver. (b) Approach maneuver.

the separation and approach phases of the maneuver (fig. 6-5). Diffraction effects contribute to uncertainty in the d_A measurements. The slopes of the lines in figure 6-5 indicate that the spacecraft separation velocity was 1.0 m/sec and that the approach velocity was 0.8 m/sec.

From 164 to 306 seconds after undocking (140 m during the separation maneuver to 185 m during the approach maneuver), all frames were "washed out" by strong reflection of earthlight from the cone of the Apollo command module. The eclipse was again observed from 306 seconds after undocking to its end at 450 seconds (70-m spacecraft separation).

TABLE 6-IV.—Photometrically Processed Frames

Series/ exposure no.	*Exposure, sec*	*Time after undocking, sec*	*Separation between spacecraft, m*	*Object*
II/4	0.33	80.0	55	Corona
II/5	.16	83.6	58	Corona
III/4	.33	115.8	90	Corona
X/3	1.1	361.8	142	RCS plume
X/4	.33	365.7	138	RCS plume
XI/4	.33	401.4	109	Corona
XII/3	1.1	433.2	83	Corona
XII/5	.16	440.1	77	Corona

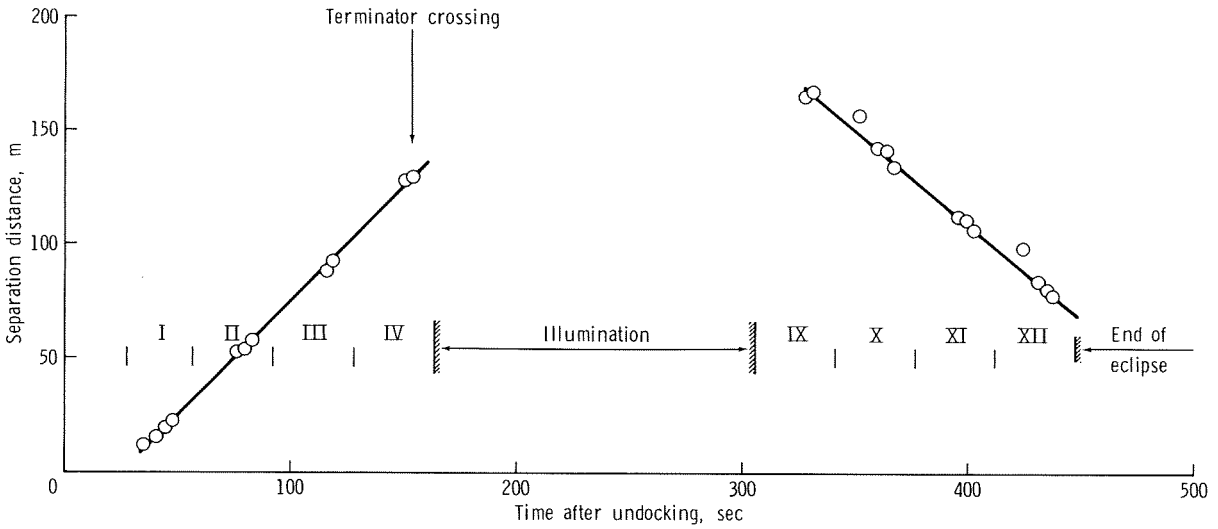

FIGURE 6-5.—The Apollo and Soyuz separation distance d as a function of time after undocking, based on measurements of the Apollo angular diameter on 24 frames. Roman numerals denote the corresponding photographic series.

PHOTOGRAPH CALIBRATION AND PRODUCTION OF ISOPHOTES

The photographs listed in table 6-IV were selected for processing. A second-order equal-density locus was constructed for seven photographs, using a photographic method with the Sabatier effect. Individual equal-density loci were combined for each photograph. Convergence was done in reference to the stars and frame boundaries. To convert these loci into isophotes, a photometric trace with a microphotometer was performed on the negatives along the Sun-Mercury line (viz., approximately along the ecliptic) to obtain the relative intensities between the equal-density loci. The absolute photometric correlation was performed on three negatives, using the star γ Geminorum as a standard (+1.8 photovisual magnitude). Since the star image was entirely contained within the aperture of the microphotometer, creating an area on the negative of $S_o = 0.1 \times 0.1$ mm^2, the density of the star image D^* was determined from the following equation.

$$D = D^* \frac{S_\gamma}{S_o} + D_\phi \left(1 - \frac{S_\gamma}{S_o}\right) \tag{6-4}$$

where D_ϕ is the background density near the star, D is the star density within the aperture, including the background, and $S_\gamma = 0.005$ mm^2 is the area of the star image. The corresponding intensity of the star was then determined from the performance curve, which was plotted from the tube photometric data. The vignetting of the lens field of view (0.5 in the γ Geminorum region of the frame) was taken into account. The absolute intensity is expressed in fractions of solar disk intensity by the ratio

$$\log \frac{i_\gamma}{i_\odot} = \log \frac{S_\odot}{S_\gamma} - 0.4(m_\gamma - m_\odot) \tag{6-5}$$
$$= -9.7$$

where the apparent photovisual magnitude of the Sun $m_\odot$ is -26.7 and the area of the Sun image $S_\odot$ is 0.5 mm^2. All the intensity determinations of the γ Geminorum image on three different negatives, each with a 0.33-second exposure, coincide to within 10 percent. The α Canis Minoris (-0.4 photovisual magnitude) star measurements were performed as controls; the results coincide to within 15 percent. Figure 6-6 shows various frame positives and associated isophotes, the originals of which were originally made on a 10:1 scale of the negatives.

PATTERN OF CORONA INTENSITY ALONG THE ECLIPTIC

As mentioned earlier, considerable illumination was coming from the OM cabin. To take this light into consideration, a frame with a 0.33-second exposure was used. This photograph was taken before undocking (series 0, frame 4) when the Soyuz hatch window was completely shaded by the Apollo spacecraft. A photometric trace was done on this frame along the ecliptic direction, and the contribution of cabin illumination to the other frames was thus determined. At an angular distance R greater than 14° from the Sun, the cabin light constitutes the entire illumination. At $R = 10°$, the cabin illumination exceeds the brightness of the corona by a factor of 3, whereas at $R < 5°$, the cabin illumination is less than one-half the total brightness. Figure 6-7 shows the corrected data on corona light intensity along the ecliptic, including corrections for the vignetting of the baffle and lens (fig. 6-8). For distances of less than 3° from the Sun, use of the frame XII/5 enabled the investigators to obtain measurements in the vicinity of $R = 1.5°$. The best fit to the corrected corona data is given by the equation

$$\frac{i}{i_\odot} = \frac{4 \times 10^{-7}}{\left(\frac{R}{R_\odot}\right)^{2.5}} \tag{6-6}$$

where $R_\odot$ is the solar radius. All the light intensities are three times higher than the known 1954 data that were obtained by Blackwell from aircraft observations (refs. 6-1 and 6-2), and it is difficult to attribute this discrepancy to errors in absolute time tagging.

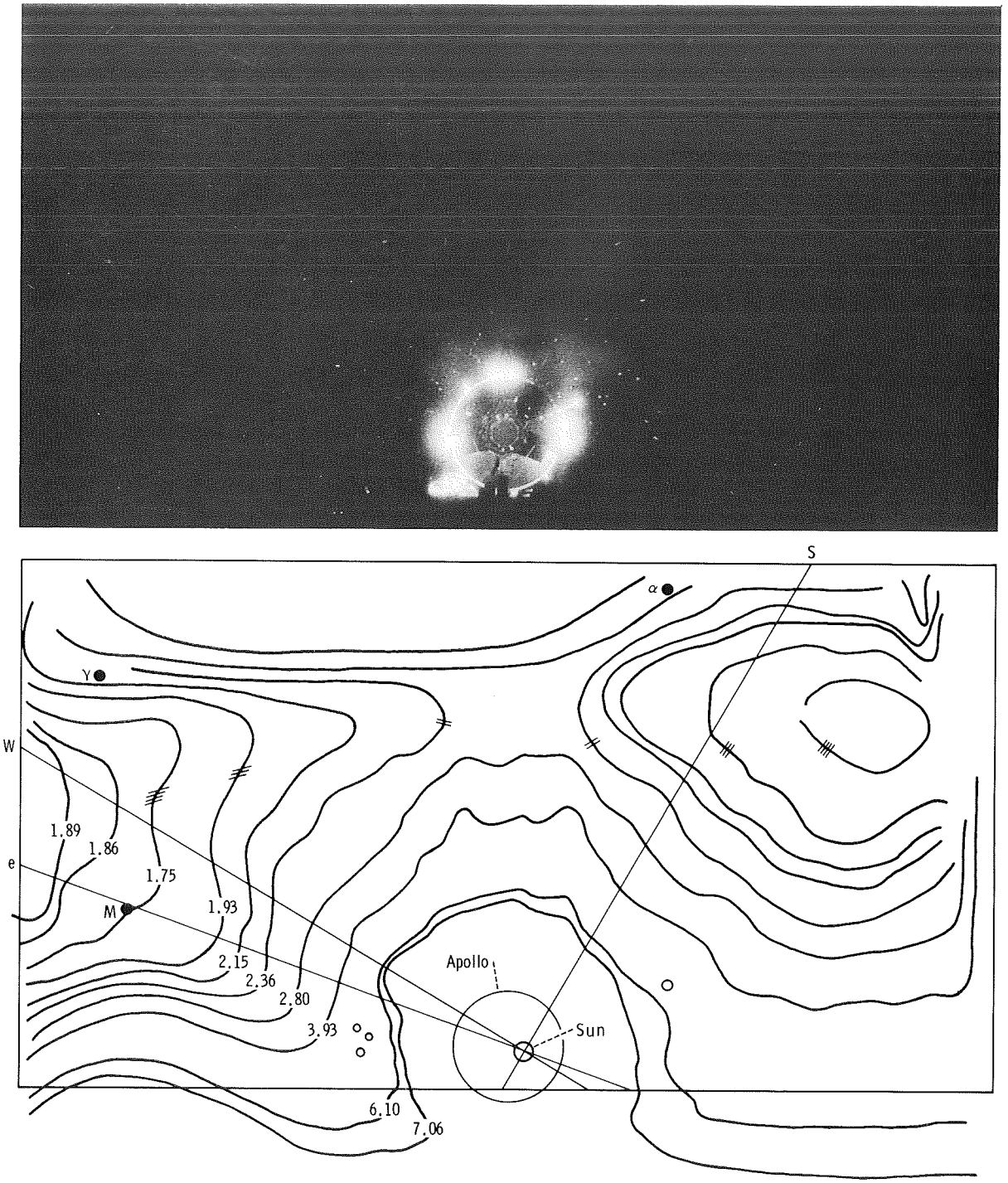

(a) Frame II/4 and isophotes.

FIGURE 6-6.—Photographic positives for designated ASE frames together with related isophote maps. Isophotes are given in 10^{-10} units of solar disk center intensity. Positions of the Sun, stars γ Geminorum (γ) and α Canis Minoris (α), planet Mercury (M), and Apollo are indicated. Directions are given for the ecliptic (e), the declination circle (S), and the orthogonal coordinate (W). The lower line indicates the hypothetical 100-percent-vignetting line of the baffle.

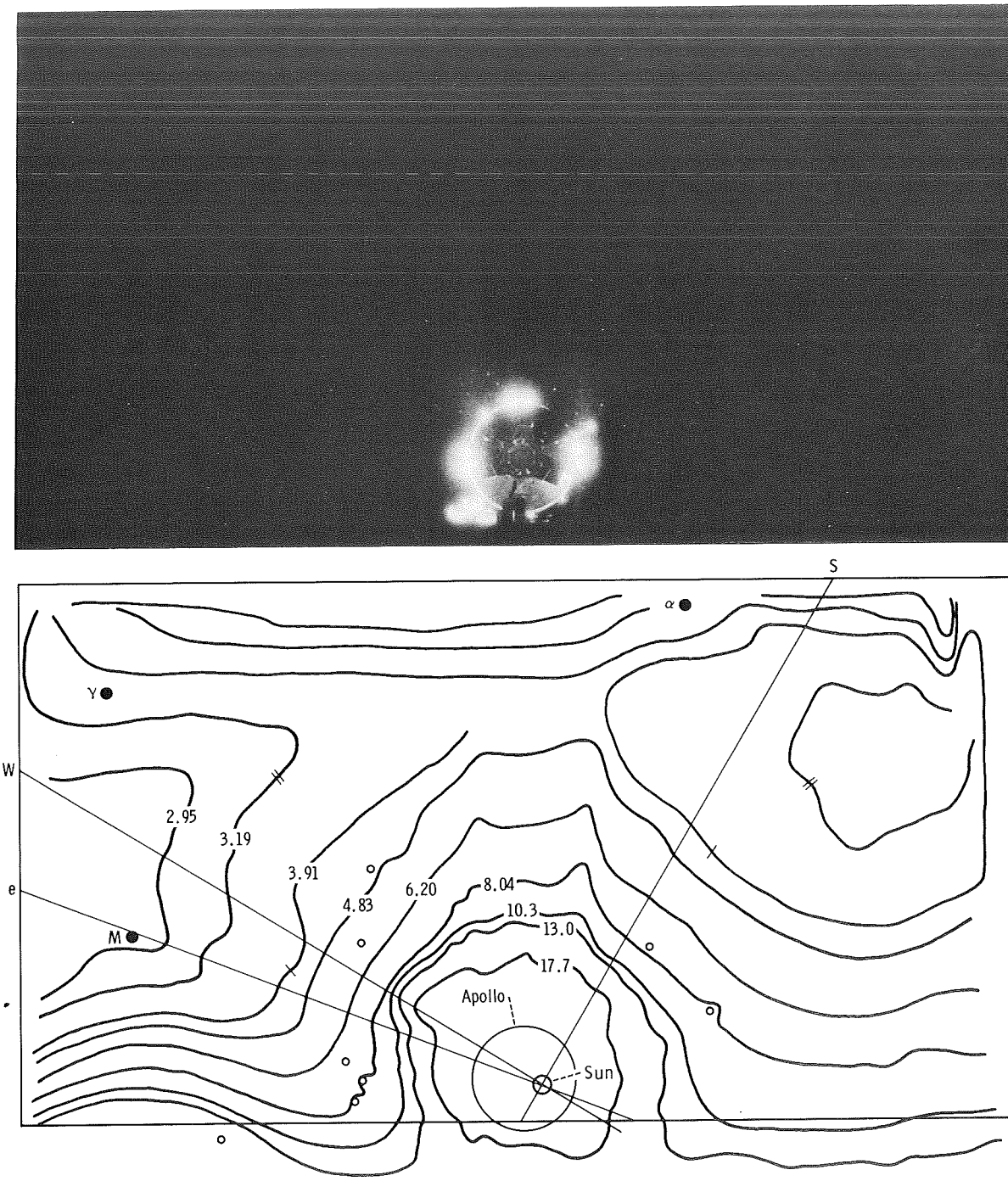

(b) Frame II/5 and isophotes.

FIGURE 6-6.—Continued.

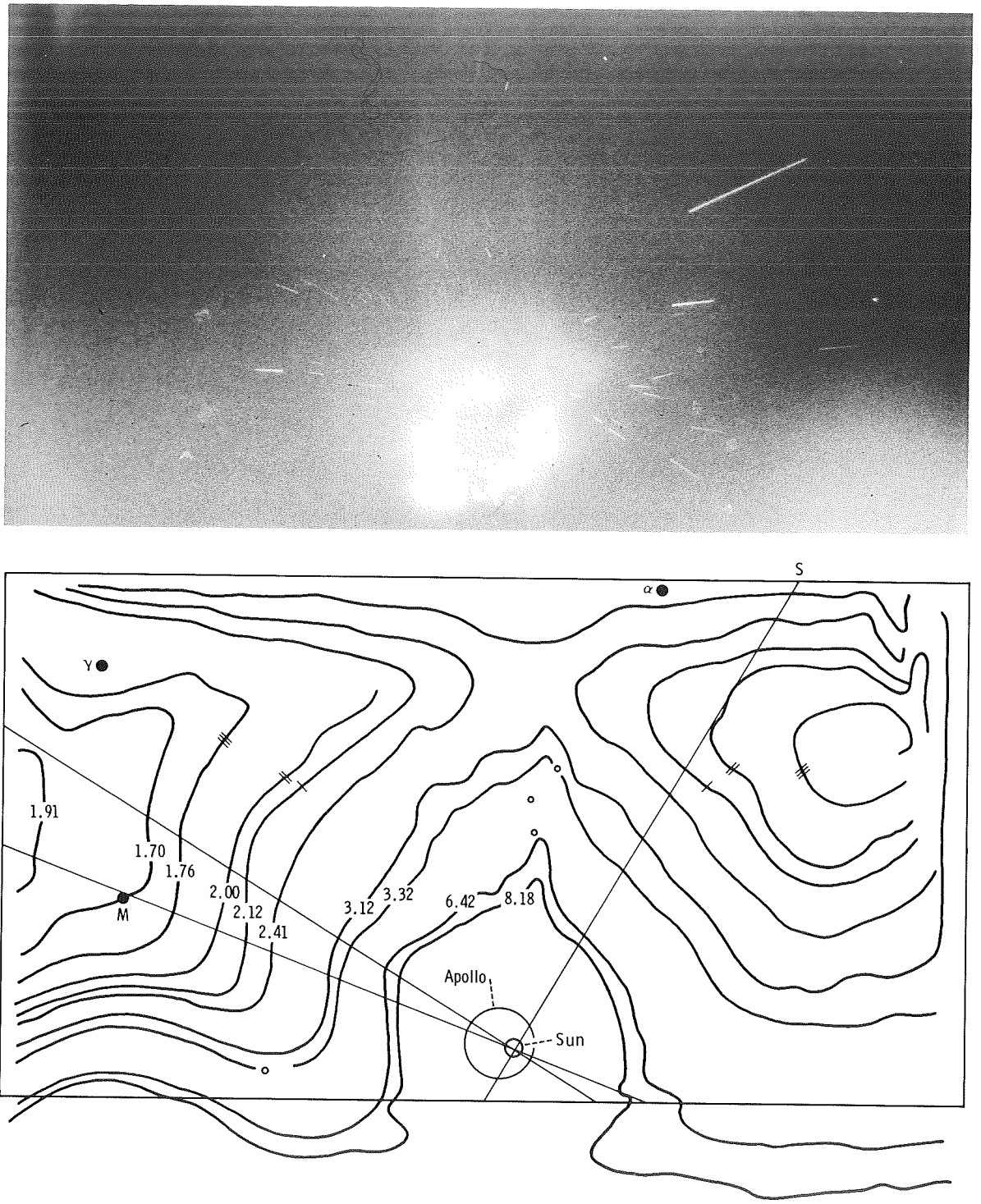

(c) Frame III/4 and isophotes.

FIGURE 6-6.—Continued.

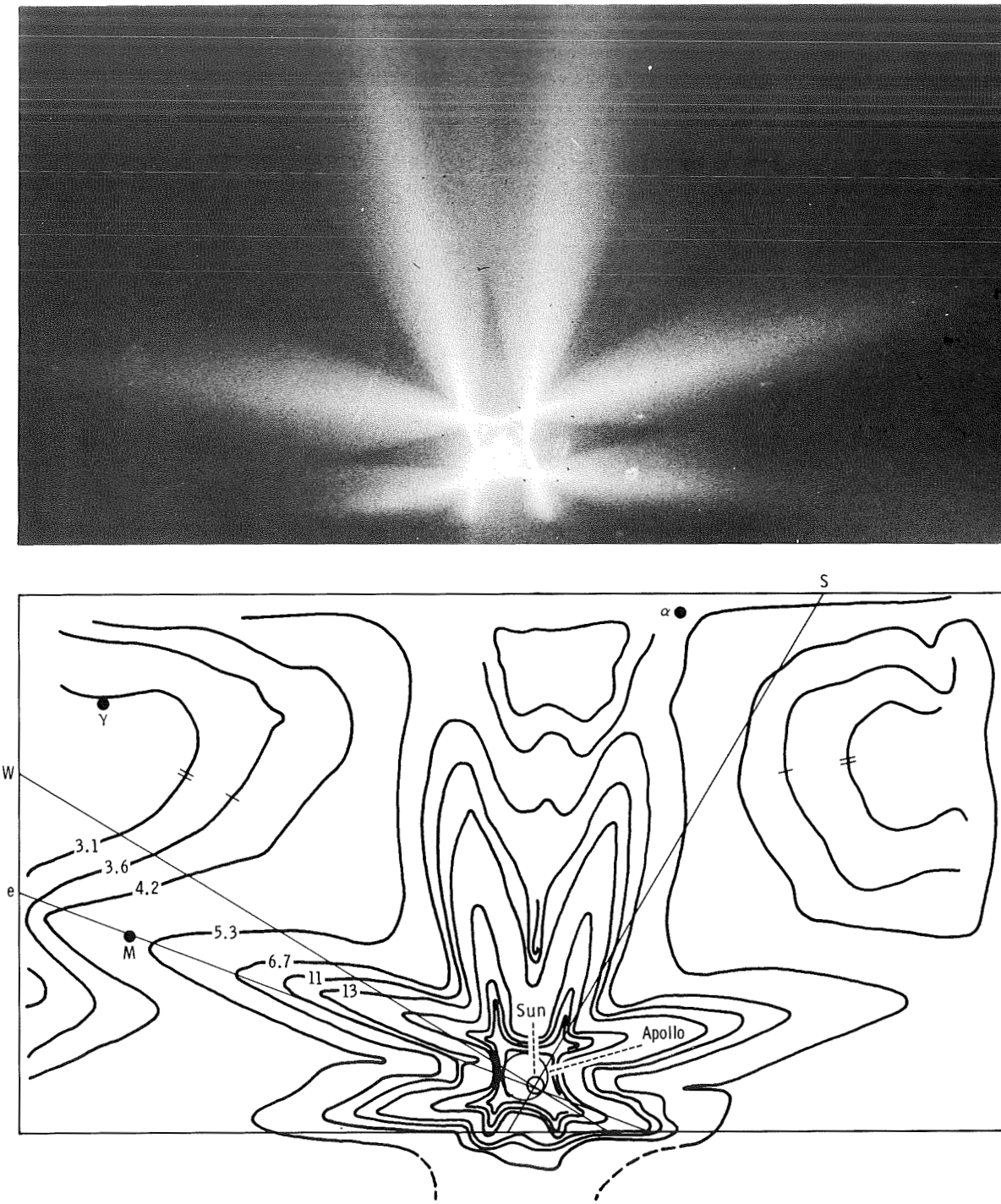

(d) Frame X/3 and isophotes.

FIGURE 6-6.—Continued.

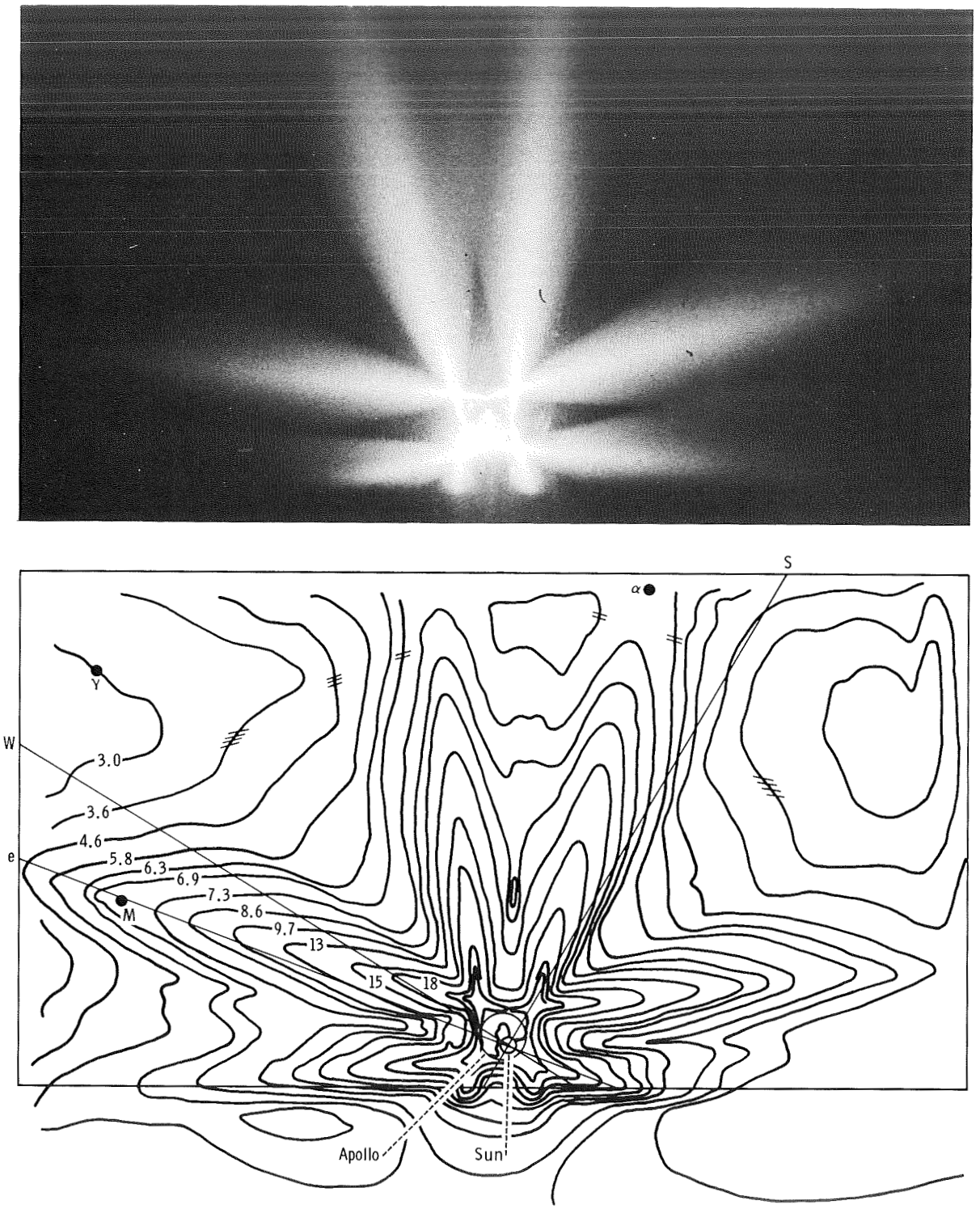

(e) Frame X/4 and isophotes.

FIGURE 6-6.—Continued.

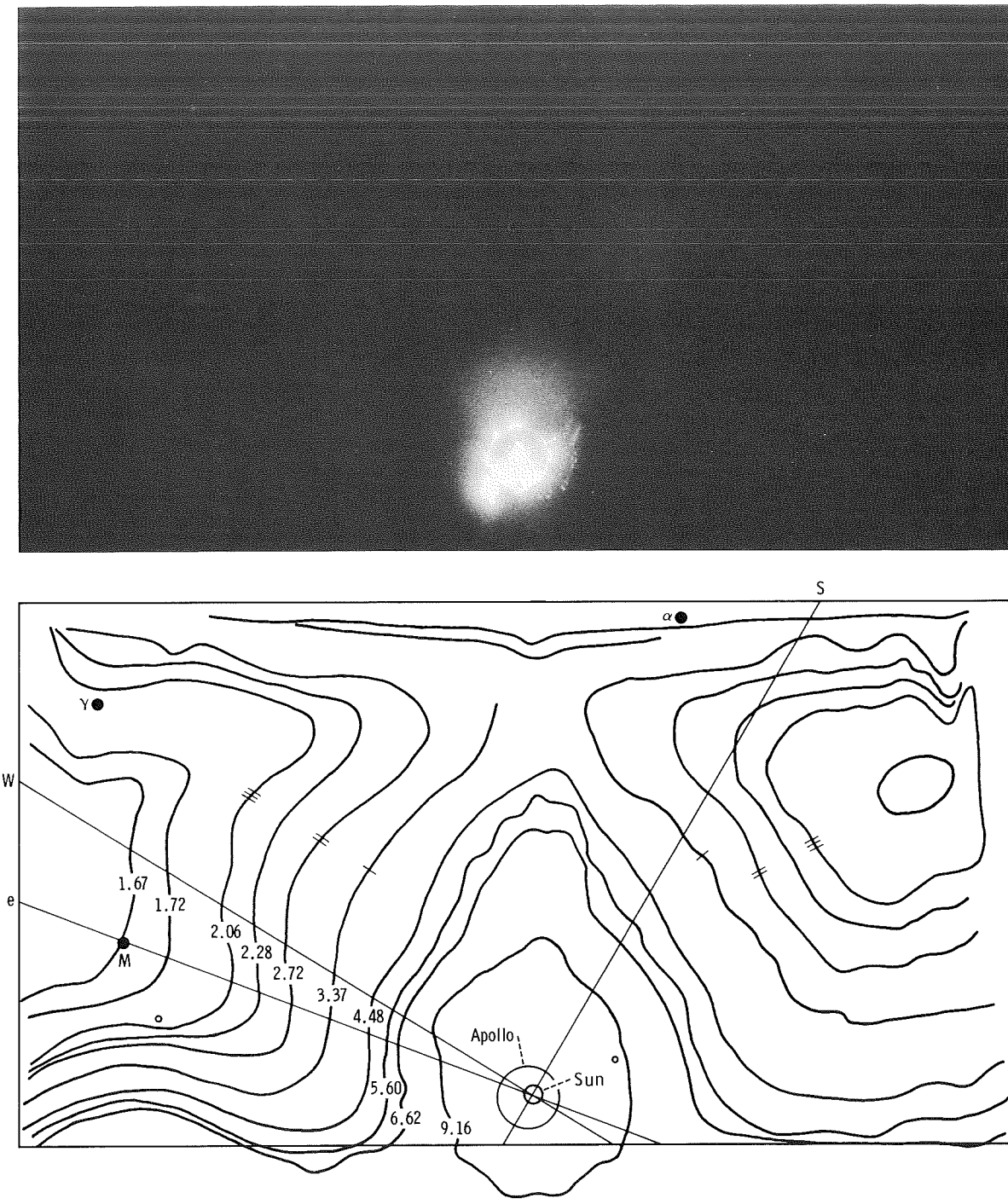

(f) Frame XI/4 and isophotes.

FIGURE 6-6.—Continued.

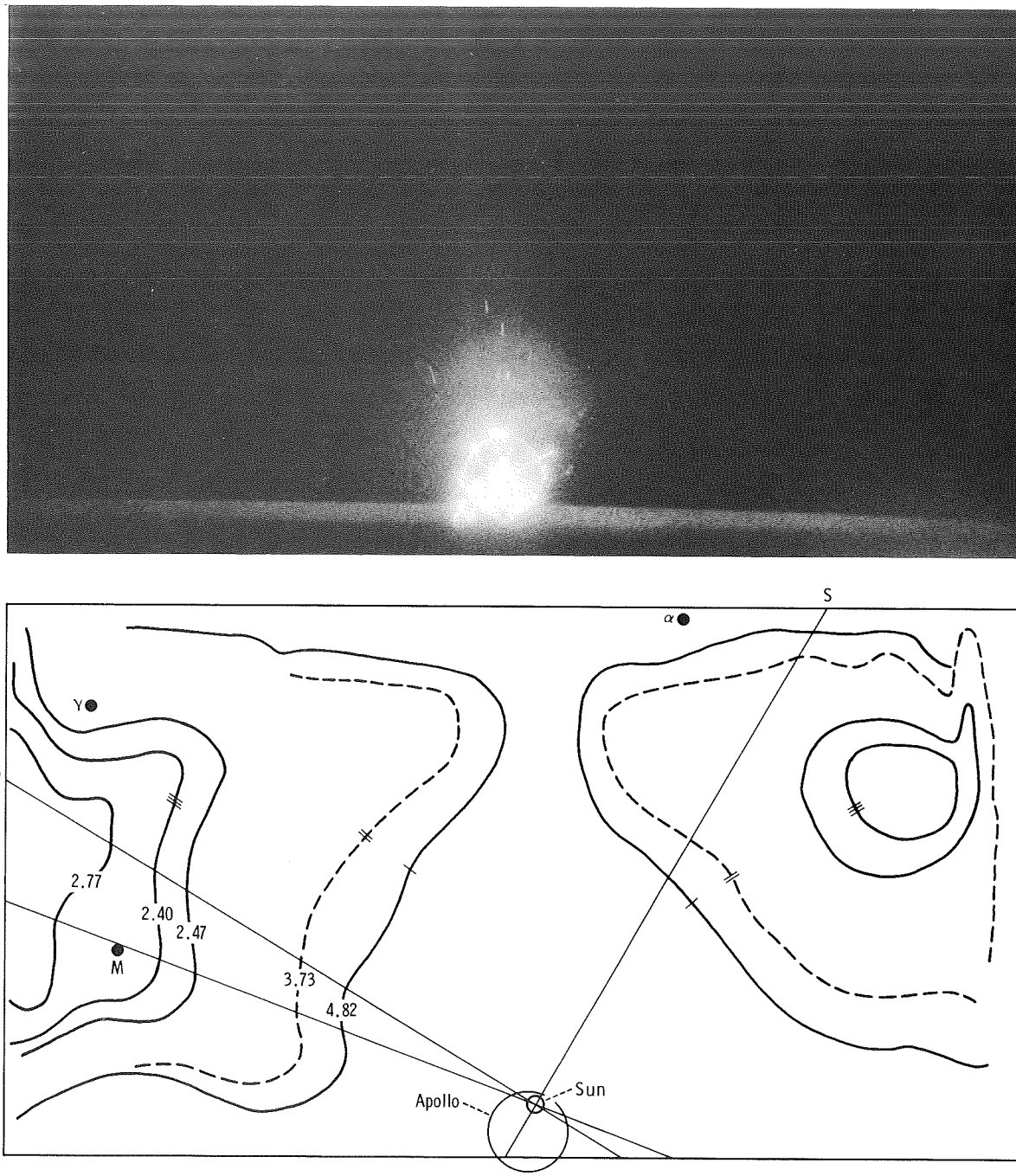

(g) Frame XII/3 and isophotes.

FIGURE 6-6.—Concluded.

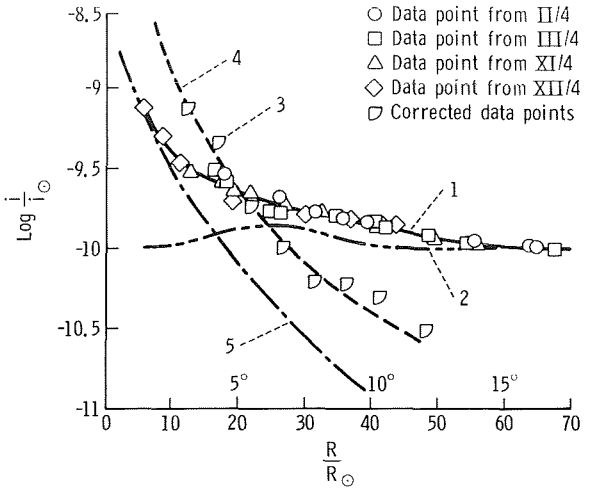

FIGURE 6-7.—Light distribution of the outer corona along the ecliptic. Number designations are as follows: 1. Light intensity distribution along the ecliptic as measured on the four indicated frames. 2. Distribution of cabin-light illumination along the ecliptic. 3. Data corrected for the cabin illumination and for lens and baffle vignetting. 4. Best fit to the corrected data (using eq. (6-6)). 5. Data obtained by Blackwell in 1954 (refs. 6-1 and 6-2).

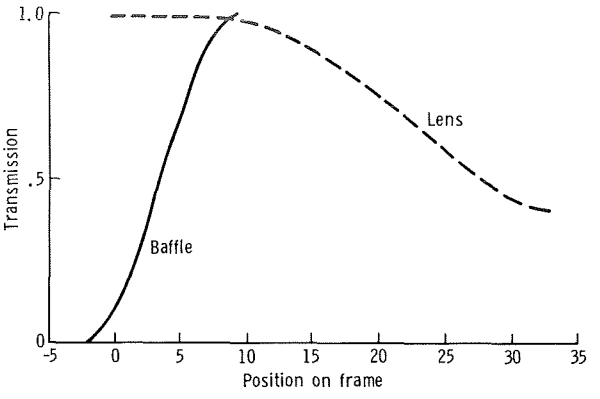

FIGURE 6-8.—Baffle and lens transmission as a function of position on the frame. The zero point is the center of a frame (optical axis of the camera). The lens vignetting curve is radially symmetric about the zero point. The baffle vignetting curve pertains only to the vertical direction; distance on the abscissa increases upward (away from the Earth). Baffle transmission is constant along any horizontal line on the frame.

CONCLUSIONS

This preliminary analysis of the ASE experiment leads to the following conclusions.

1. The ASE experiment demonstrated that it was an effective method for studying the spatial distribution of contaminants produced by RCS engines as they function in a vacuum and in the gas-dust "atmosphere" that surrounds the space vehicles.

2. The atmosphere surrounding the space vehicle is a serious obstacle in performing observations of the dimly lit astronomical objects. This atmosphere is created, primarily, by the gas evaporation and particle condensation originating from the RCS engines.

3. Perhaps the major result of the ASE experiment is its demonstration that the simulation of solar eclipse is possible by providing an "artificial Moon" at a distance of approximately 100 m. Although diffraction phenomena on the artificial Moon did occur, they did not interfere with the observation of the outer corona. However, to obtain reliable quantitative data, it is essential to use a "clean" artificial Moon that does not discharge gas or particles.

REFERENCES

6-1. Blackwell, D. E.: A Study of the Outer Corona From a High Altitude Aircraft at the Eclipse of 1954 June 30. Monthly Notices Roy. Astron. Soc., vol. 115, no. 6, 1955, pp. 629-649.

6-2. Blackwell, D. E.; Ingham, M. F.; and Dewhirst, D. W.: The Zodiacal Light. Advances in Astronomy and Astrophysics, Zdeněk Kopal, ed., vol. 5, Academic Press, Inc. (New York), 1967, pp. 1-69.